Multimessenger Picture of the FSRQ J1048+7143

Emma Kun,[a,b,c,d,e,*] **Ilja Jaroschewski,**[b,c] **Armin Ghorbanietemad,**[b,c] **Sándor Frey,**[d,e,f] **Julia Becker Tjus,**[b,c,g] **Silke Britzen,**[h] **Krisztina Éva Gabányi,**[d,e,i,j] **Vladimir Kiselev,**[b,c] **Leander Schlegel,**[b,c] **Marcel Schroller,**[b,c] **Lang Cui,**[k] **Xin Wang,**[k] **Yuling Shen**[k] **and Patrick Reichherzer**[l]

[a]*Astronomical Institute, Faculty for Physics & Astronomy, Ruhr University Bochum, 44780 Bochum, Germany*

[b]*Theoretical Physics IV: Plasma-Astroparticle Physics, Faculty for Physics & Astronomy, RUB, 44780 Bochum, Germany*

[c]*Ruhr Astroparticle And Plasma Physics Center (RAPP Center), RUB, 44780 Bochum, Germany*

[d]*Konkoly Observatory, ELKH Research Centre for Astronomy and Earth Sciences, Konkoly Thege Miklós út 15-17, H-1121 Budapest, Hungary*

[e]*CSFK, MTA Centre of Excellence, Konkoly Thege Miklós út 15-17, H-1121 Budapest, Hungary*

[f]*Institute of Physics, ELTE Eötvös Loránd University, Pázmány Péter sétány 1/A, H-1117 Budapest, Hungary*

[g]*Department of Space, Earth and Environment, Chalmers University of Technology, 412 96 Gothenburg, Sweden*

[h]*Max-Panck-Institut für Radioastronomie, Auf dem Hügel 69, 53121 Bonn, Germany*

[i]*Department of Astronomy, Eötvös Loránd University, Pázmány Péter sétány 1/A, H-1117 Budapest, Hungary*

[j]*ELKH-ELTE Extragalactic Astrophysics Research Group, Pázmány Péter sétány 1/A, H-1117 Budapest, Hungary*

[k]*Xinjiang Astronomical Observatory, Chinese Academy of Sciences, 150 Science 1-Street, Urumqi 830011, People's Republic of China*

[l]*Department of Physics, University of Oxford, Oxford OX1 3PU, United Kingdom*

E-mail: kun.emma@csfk.org

In this paper we present the multimessenger picture of the flat-spectrum radio quasar (FSRQ) J1048+7143, a blazar showing gamma-ray quasi-periodic oscillations. We generate the adaptively binned Fermi-LAT light curve of this source above 168 MeV and find three major γ-ray flares, such that each of the flares resolves into two subflares. By analyzing arcsec-scale and milliarcsec-scale radio interferometric observations, we find signatures of the precession of a spine–sheath structured jet. We analyze the 5 GHz total flux density curve of J1048+7143 taken with single-dish radio telescopes, and find three complete radio flares that are also suggestive of jet precession. We model the timing of gamma-ray flares as a signature of the spin-orbit precession in a supermassive black hole binary and find that the binary could merge in the next 60–80 yrs.

*Speaker

1. Introduction

Active galactic nuclei (AGN) are driven by supermassive black holes (SMBHs) in their center, with up to billions of solar masses. Observations on AGN reveal such objects at distances corresponding to only a few percent of the current age of the Universe [e.g. 12]. Since measurements on high-energy γ-rays [e.g. 11, 14] and cosmic rays [e.g. 28] have horizons and are scrambled, only neutrinos could pinpoint those massive celestial particle accelerators. Observation of quasi-periodic neutrino emission might be the only direct evidence if such distant AGN has a periodic nature, e.g. due to precessing SMBH binaries (SMBBHs).

Detection of gravitational radiation of SMBBHs will be a new direct way to find merging SMBHs, at present there are only indirect ways to find them. In a radio-loud AGN, a periodic jet structure might indicate that the jet emitter black hole interacts gravitationally with another black hole [e.g. 18]. Very long baseline interferometry (VLBI) provides a great tool to study AGN jets on pc scales (e.g., [21]) and to find periodic jets [e.g. 7, 9, 18, and references therein].

In the interpretation of quasi-periodic oscillations due to jet precession induced by a SMBBH system, [10] built a precession model to explain the recurrent neutrino emission in TXS 0506+056 observed by the Antarctic IceCube Neutrino Observatory [16, 17]. They connected for the first time the possible neutrino and gravitational-wave signatures of such sources, demonstrating the need for continued multi-messenger monitoring [29]. This precession model predicted a new neutrino emission period that turned out to be consistent with the 18/09/2022 neutrino observation by IceCube and relied on the jet precession first reported by [8] for this source. [5] showed that the neutrino cadence of TXS 0506+056 is consistent with an SMBBH origin.

Quasi-periodic oscillations (QPOs) can be detected in optical, X-ray, radio bands and in a few cases also in the γ-ray regime [e.g. 30]. Recently, [34] generated the 5-day binned gamma-ray light curve of 4FGL J1048.4+7143 and found a possible QPO with a period of 3.06 ± 0.43 yr at the significance level of $\sim 3.6\sigma$. J1048+7143 is a low-synchrotron-peaked flat-spectrum radio quasar (FSRQ) at redshift $z = 1.15$ [27], associated with the Fermi γ-ray source 4FGL 1048.4+7143 [1, 3]. We generate and model the adaptively binned γ-ray light curve of this source. We also analyze kpc- and pc-scaled VLBI observations and single dish flux density curves. Expanding the precession model of [10], in this paper we propose the multimessenger picture of J1048+7143 assuming that the flaring activity of this source is due to the spin–orbit precession [13] of a SMBBH at its heart.

2. The γ-ray light curve analysis of J1048+7143

We obtained archival data taken with the Large Area Telescope (LAT) instrument onboard the Fermi Gamma-ray Space Telescope to generate the γ-ray light curve of 4FGL J1048.4+7143. This bright γ-ray source ($RA_{J2000} = 162.1067°$, $DEC_{J2000} = 71.7297°$ [4FGL, 1]) is associated with the FSRQ 6C 104451+715930 (hereafter J1048+7143). We analyzed almost 14 years of Fermi-LAT data (2008 Aug 4 – 2022 Mar 14) in the energy range $100\,\text{MeV} - 800\,\text{GeV}$. We performed the binned likelihood analysis of the data using the fermipy v1.0.1 and ScienceTools v2.0.8 packages (see the description of the technical details in [20]). We applied an adaptive-binning algorithm [23] to set the bin widths of the light curve to study the flaring activity of this blazar. We compute the
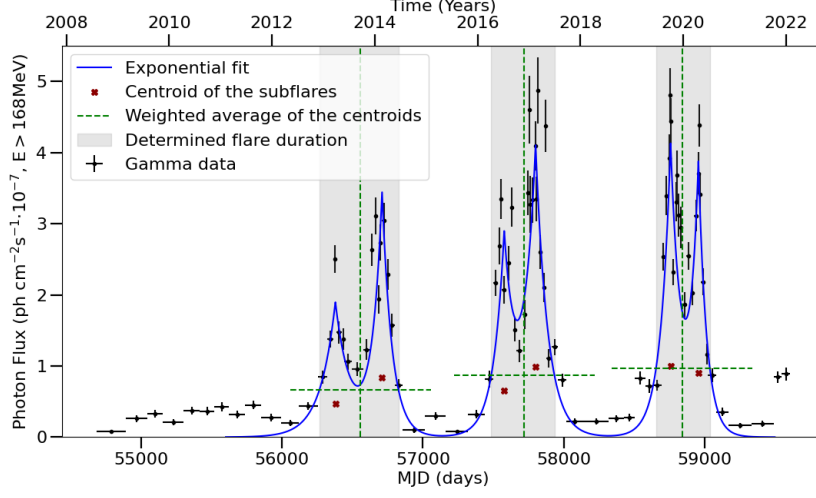
Figure 1: The γ-ray flux curve of J1048+7143. The sum of the contributions of the exponential flares fitted to the light curve is shown by a blue continuous line. Centroids of the three major flares ($E > 168$ MeV) are marked by green horizontal and vertical dashed lines.

Table 1: Exponential fitting of the γ-ray light curve of 4FGL J1048.4+7143. See the description of the parameters in the text.

Parameter	$F_{1,1}$	$F_{1,2}$	$F_{2,1}$	$F_{2,2}$	$F_{3,1}$	$F_{3,2}$
a ($\times 10^{-7}$ ph cm^{-2}s^{-1})	1.87 ± 0.40	3.36 ± 0.64	2.60 ± 0.70	3.97 ± 0.60	4.01 ± 0.58	3.63 ± 0.62
b (MJD, days)	56378 ± 17	56710 ± 10	57578 ± 15	57801 ± 10	58760 ± 8	58957 ± 7
c (days)	109 ± 32	70 ± 17	75 ± 23	87 ± 17	72 ± 14	58 ± 13

light curve above 168 MeV to optimize the accumulation times and to avoid the accidental capture of background photons.

We plot the photon flux of 4FGL J1048.4+7143 as function of time in Fig. 1. The source was in a quiescent phase till about MJD 56000 and after that the source has shown three major flares with subflare structure. We fitted the light curve with two-sided exponential functions in the form of

$$F_{i,j}(t) = a_0 + a_{i,j} \times \exp\left[\frac{-|t - b_{i,j}|}{c_{i,j}}\right], \tag{1}$$

with t being the time, the index i running from 1 to 3 for the three main flares, j is 1 or 2 for the subflares of the ith main flares, a_0 measuring the baseline, $a_{i,j}$ the height, $b_{i,j}$ the time location of the peak, and $c_{i,j}$ the slope of the exponential function. The resulting fit parameters are shown in Table 1 ($\chi^2_{\rm red} \approx 11.2$).

Employing the so-called centroid method, we determined the centers of the three major γ-ray flares as MJDs 56556 ± 69, 57720 ± 53, 58843 ± 44, and consequently the flare duration in days as 561 ± 81, 449 ± 89, 383 ± 57. The inferred flare durations are marked as gray areas in Fig. 1. The elapsed time between the centers of corresponding major flares are $P_{1\to2} = 3.19 \pm 0.24$ yr (the time interval between major flare one and two) and $P_{2\to3} = 3.07 \pm 0.19$ yr (the time interval between major flare two and three).
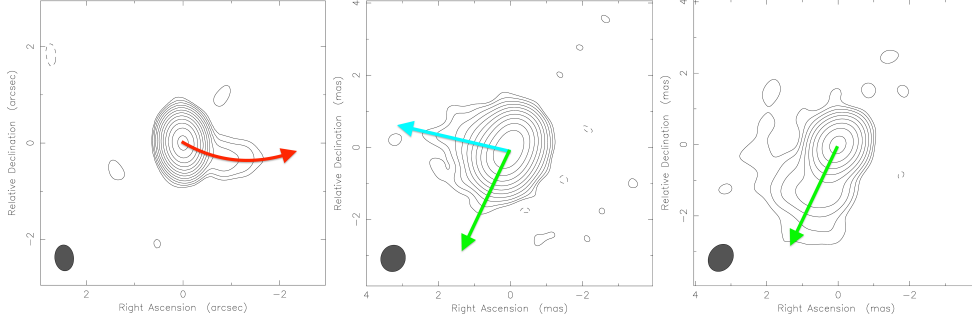
Figure 2: *Left:* The jet of J1048+7143 as seen at 4.8-GHz with the VLA. The jet is oriented towards west and it extends to ∼ 15 kpc projected distance (red arrow). *Middle and right:* Two examples of the 8.6-GHz jet structure observed with the VLBI (observing dates 2001 Jul 7 and 2010 Mar 23, respectively). In the mas-scale structure (8.361 pc/mas), there is an approximately eastern (turquoise arrow) and a southern jet extension (green arrow), such that sometimes the eastern and sometimes the southern jet dominates.

3. Signatures of jet precession on the kpc- and pc-scale radio structure of J1048+7143

We chose the Very Large Array (VLA) imaging experiment AG512 (PI: L. Greenhill) conducted on 1997 Jan 12 to reveal the kpc-scale structure of J1048+7143. The data are available in the U.S. National Radio Astronomy Observatory (NRAO) archive[1]. The FSRQ J1048+7143 was the calibrator source for observing the water megamaser in NGC 3735 [15] at 4.8, 8.4, and 15 GHz frequencies. We present the 4.8-GHz image of J1048+7143 in Fig. 2, left.

We employed archival (calibrated) 8.6-GHz visibility data obtained with the Very Long Baseline Array (VLBA), sometimes augmented with other radio telescopes, to derive the structural properties of the pc-scale jet of J1048+7143. The observations were carried out between 1994.61 and 2020.73, spanning more than 26 yr at 69 epochs[2]. See the details about the analysis of archival VLA and VLBA observations in [20].

In the middle panel of Fig. 2 (observing date 2001 Jul 5), we see a jet pointing approximately toward east and one pointing south. In the right panel of the same Fig. 2, at another epoch (2010 Mar 23), we see only a south-directed jet. This, also considering the large misalignment between the arcsec- and mas-scale jets, suggests jet precession in the source.

We show archival 4.8-GHz single dish flux density curves of J1048+7143 in Fig. 3., obtained with the Nanshan 26-m radio telescope [e.g. 22] and with the 600-m RATAN-600 radio telescope [24]. After a quiescence phase, the single dish flux density curves reveal 2–3 major radio flares of this blazar at 4.8 GHz, such that their peaks clearly coincide with the centroids of the major γ-ray flares.

4. Spin–orbit precession in J1048+7143

Spin-orbit precessing SMBH jets [e.g. 19] can be revealed by quasi-periodic flaring emissions. We test for the (quasi-) periodic behavior of the three major flares (see in Fig. 1) for this scenario.

---

[1] https://data.nrao.edu/

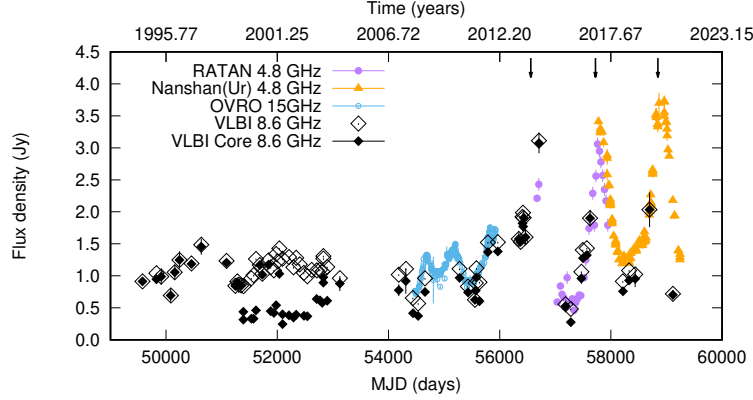[2] http://astrogeo.org/cgi-bin/imdb_get_source.csh?source=J1048%2B7143

Figure 3: The RATAN-600 4.8-GHz (purple filled circles), Nanshan 4.8-GHz (orange triangles), OVRO 15-GHz single-dish radio flux density curves (blue empty diamonds), the 8.6-GHz integrated interferometric flux density of J1048+7143 (black empty diamonds), and the 8.6-GHz flux density of the VLBI core (black filled diamonds). We plot the time coordinate of centroids of the three major γ-ray flares by down-pointing black arrows.

We expand the jet precession model of [10], which determines the direction angle of dominant spin, ϕ [changes from $0°$ to $360°$, see in 10] as a function of the remaining time until the binary coalescence, ΔT_{GW}. This model is valid in the 2.5 post-Newtonian (PN)([13]). We modified the model of [10] by allowing small mass ratios, $q = m_2/m_1 < 1 (m_1 + m_2 = M)$, of the binary that results in

$$\phi(\Delta T_{\mathrm{GW}}, q) = -\frac{2(4+3q)}{(1+q)^2}\left(\frac{5\,c}{32\,G^{1/3}M^{1/3}} \cdot \frac{(1+q)^2}{q}\right)^{3/4}(\Delta T_{\mathrm{GW}})^{1/4} + \psi, \qquad (2)$$

where G is the gravitational constant, M is the total mass of the SMBBH, c is the speed of light, and ψ is an integration constant, which defines the initial direction of the jet. We use the one-spin formalism of [13] and assume the direction of the jet to be parallel with the dominant spin (see the reasoning e.g. in [18]).

Thus, we can establish the connection between two consecutive flares as they reveal one complete spin-orbit precession period (P_{jet}):

$$\phi(\Delta T_{\mathrm{GW}}, q) = \phi(\Delta T_{\mathrm{GW}} - P_{\mathrm{jet}}, q) \pm \zeta. \qquad (3)$$

During one precession period, the time remaining until the binary coalescence decreases from ΔT_{GW} to $\Delta T_{\mathrm{GW}} - P_{\mathrm{jet}}$, such that ζ identifies as the half-opening angle of the jet. Employing Eqs. (2)-(3), we determine the remaining merger time of the SMBBH. Possible values for the merger time as function of the mass ratio q are shown in the left side of Fig. 4. We constrain the range of possible mass ratios to the typical mass ratio values of merging SMBBHs ($q = 1/3$–$q = 1/30$) [13], adopting a total mass of $10^{9.16\pm0.2}\,M_\odot$ [26] at redshift $z = 1.15$ [27]. The predicted time of the merger (as seen from Earth) can be seen by green. Invalid mass ratios ($q \gtrsim 1/4$) based on the third major γ-ray flare are highlighted by the red area. From this we conclude the binary could merge in the next ~ 60 to 80 yrs. Using our model we predict that fourth flare of J1048+7143 will occur before the end of 2024, at the latest before summer 2025.
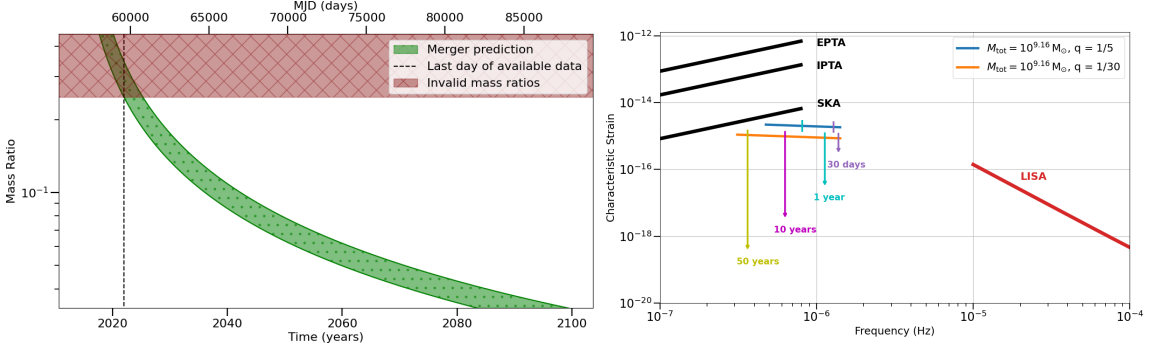
5

Figure 4: Left: Time of the merger of the hypothetical SMBBH at the center of J1048+7143, as a function of its mass ratio. Right: Gravitational wave signals from J1048+7143 assuming a SMBBH merger at its core. The blue and orange lines show the expected characteristic strain with the mass ratio $q = 1/5$ and $q = 1/30$, respectively. The black lines show the sensitivity curves from the detectors SKA, IPTA and EPTA [25]. The red line shows the LISA sensitivity curve, while other colored lines indicate the gravitational wave frequency emitted by a possible binary with (from left to right) 50 years (yellow), 10 years (magenta), 1 year (cyan), and 30 days (purple).

5. Gravitational wave signal expected from J1048+7143

As we have shown, the γ-ray signals from J1048+7143 are consistent with a SMBBH merger at its core. Now we determine the gravitational wave (GW) signal expected from the source. We model the expected characteristic strain h_c as [31]:

$$ h_c = \sqrt{\frac{2}{3}} \frac{1}{r(z)} \frac{1}{\pi^{2/3}c^{3/2}} \frac{(G\mathcal{M})^{5/6}}{(1+z)^{1/2}} f^{-1/6} , \tag{4} $$

with the co-moving source distance $r(z)$, the chirp mass $\mathcal{M} = (m_1 m_2)^{3/5}/(m_1 + m_2)^{1/5}$ and the observed GW frequency f. The corresponding GW frequencies range from arbitrary small frequencies to f_{ISCO}, which describes the emitted GW frequency at the innermost stable circular orbit [ISCO, see e.g. 33]. We plot the expected characteristic strain in the right side of Fig. 4 for the limiting mass ratios $q = 1/5$ (blue) and $q = 1/30$ (orange). Setting the remaining time until the final coalescence for 50, 10, 1 year and 30 days, we determined the frequencies of gravitational waves emitted from this source [6, 33]. These GW frequencies are indicated with vertical dashes in the colors (from left to right) yellow, magenta, cyan, and purple in the right side of Fig. 4. Sensitivity curves from the European Pulsar Timing Array (EPTA), International Pulsar Timing Array (IPTA), and Square Kilometer Array (SKA) are shown in black [25] in the same figure, while the LISA sensitivity curve [2] is shown in red. Fig. 4 shows that neither the PTAs nor LISA can detect J1048+7143 in gravitational waves.

The multiwavelength behavior of J1048+7143 is qualitatively compatible with a spine-sheath jet periodically crossing a target close to our line of sight (e.g. clouds of the broad-line region), where the outer layer, the sheath, consists of protons, electrons, positrons, while the inner jet, the spine, contains only electrons and positrons. When the sheath meets the target we expect elevated gamma-ray flux (gamma-ray subflares) and high-energy neutrinos, while from the spine crossing the target we expect only elevated radio emission peaking between the gamma-ray subflares. Finally

we note that constructing the multimessenger picture of active galaxies is key to understanding the high-energy emission from these sources [4, 10] and to find possible candidates of periodic high-energy neutrino emission.

Acknowledgments

References

[1] Abdollahi, S., Acero, F., Ackermann, M., et al. 2020, ApJS, 247, 33, doi: 10.3847/1538-4365/ab6bcb

[2] Amaro-Seoane, P., Audley, H., Babak, S., et al. 2017, arXiv e-prints, arXiv:1702.00786. https://arxiv.org/abs/1702.00786

[3] Ballet, J., Burnett, T. H., Digel, S. W., & Lott, B. 2020, arXiv e-prints, arXiv:2005.11208. https://arxiv.org/abs/2005.11208

[4] Becker, J. K. 2008, PhysRep, 458, 173, doi: 10.1016/j.physrep.2007.10.006

[5] Becker Tjus, J., Jaroschewski, I., Ghorbanietemad, A., et al. 2022, ApJ, 241, 25, doi: 10.3847/2041-8213/aca65d

[6] Berti, E., Buonanno, A., & Will, C. M. 2005, Phys. Rev. D, 71, 084025, doi: 10.1103/PhysRevD.71.084025

[7] Britzen, S., Kudryavtseva, N. A., Witzel, A., et al. 2010, A&A, 511, A57, doi: 10.1051/0004-6361/20079267

[8] Britzen, S., Fendt, C., Böttcher, M., et al. 2019, A&A, 630, 103, doi: 10.1051/0004-6361/201935422

[9] Britzen, S., Zajaček, M., Gopal-Krishna, et al. 2023, ApJ, 951, 106, doi: 10.3847/1538-4357/accbbc

[10] de Bruijn, O., Bartos, I., Biermann, P. L., & Tjus, J. B. 2020, ApJL, 905, L13, doi: 10.3847/2041-8213/abc950

[11] Dermer, C. D., Razzaque, S., Finke, J. D., & Atoyan, A. 2009, New Journal of Physics, 11, 065016, doi: 10.1088/1367-2630/11/6/065016

[12] Frey, S., Paragi, Z., Gurvits, L. I., Cseh, D., & Gabányi, K. É. 2010, A&A, 524, A83, doi: 10.1051/0004-6361/201015554

[13] Gergely, L. Á., & Biermann, P. L. 2009, Astroph. Journal, 697, 1621, doi: 10.1088/0004-637X/697/2/1621

[14] Gilmore, R. C., Somerville, R. S., Primack, J. R., & Domínguez, A. 2012, MNRAS, 422, 3189, doi: 10.1111/j.1365-2966.2012.20841.x

[15] Greenhill, L. J., Herrnstein, J. R., Moran, J. M., Menten, K. M., & Velusamy, T. 1997, ApJL, 486, L15, doi: 10.1086/310824

[16] IceCube Collaboration, Fermi-LAT, MAGIC, et al. 2018, Science, 361, 147, doi: 10.1126/science.aat1378

[17] IceCube Collaboration. 2018, Science, 361, 147, doi: 10.1126/science.aat2890

[18] Kun, E., Gabányi, K. É., Karouzos, M., Britzen, S., & Gergely, L. Á. 2014, MNRAS, 445, 1370, doi: 10.1093/mnras/stu1813

[19] Kun, E., Frey, S., & Gabányi, K. É. 2020, MNRAS, 496, 3336, doi: 10.1093/mnras/staa1734

[20] Kun, E., Jaroschewski, I., Ghorbanietemad, A., et al. 2022, ApJ, 940, 163, doi: 10.3847/1538-4357/ac9cce

[21] Lister, M. L., Homan, D. C., Hovatta, T., et al. 2019, ApJ, 874, 43, doi: 10.3847/1538-4357/ab08ee

[22] Liu, X., Mi, L. G., Liu, J., et al. 2015, A&A, 578, A34, doi: 10.1051/0004-6361/201424854

[23] Lott, B., Escande, L., Larsson, S., & Ballet, J. 2012, A&A, 544, A6, doi: 10.1051/0004-6361/201218873

[24] Mingaliev, M. G., Sotnikova, Y. V., Udovitskiy, R. Y., et al. 2014, A&A, 572, A59, doi: 10.1051/0004-6361/201424437

[25] Moore, C. J., Cole, R. H., & Berry, C. P. L. 2015, Classical and Quantum Gravity, 32, 015014, doi: 10.1088/0264-9381/32/1/015014

[26] Paliya, V. S., Domínguez, A., Ajello, M., Olmo-García, A., & Hartmann, D. 2021, ApJS, 253, 46, doi: 10.3847/1538-4365/abe135

[27] Polatidis, A. G., Wilkinson, P. N., Xu, W., et al. 1995, ApJS, 98, 1, doi: 10.1086/192152

[28] Reichherzer, P., Merten, L., Dörner, J., et al. 2022, SN Applied Sciences, 4, 15, doi: 10.1007/s42452-021-04891-z

[29] Reichherzer, P., Schüssler, F., Lefranc, V., et al. 2023, Galaxies, 11, 1, doi: 10.3390/galaxies11010022

[30] Ren, H. X., Cerruti, M., & Sahakyan, N. 2022, arXiv e-prints, arXiv:2204.13051. https://arxiv.org/abs/2204.13051

[31] Sesana, A. 2016, PRL, 116, 231102, doi: 10.1103/PhysRevLett.116.231102

[32] Shu, F., Petrov, L., Jiang, W., et al. 2017, ApJS, 230, 13, doi: 10.3847/1538-4365/aa71a3

[33] Vecchio, A. 2004, PRD, 70, 042001, doi: 10.1103/PhysRevD.70.042001

[34] Wang, G. G., Cai, J. T., & Fan, J. H. 2022, ApJ, 929, 130, doi: 10.3847/1538-4357/ac5b08

PoS(ICRC2023)1587